High-Resolution ^{31}P Field Cycling NMR as a Probe of Phospholipid Dynamics

Mary F. Roberts[†] and Alfred G. Redfield*[,‡]

*Contribution from the Department of Chemistry, Boston College,
Chestnut Hill, Massachusetts 02467, and Department of Biochemistry, Brandeis University,
Waltham, Massachusetts 02454*

Received June 7, 2004; E-mail: redfield@brandeis.edu

Abstract: We have used high-resolution field-cycling ^{31}P NMR spectroscopy to measure spin−lattice relaxation rates ($R_1 = 1/T_1$) of multicomponent phospholipid vesicle and micelle samples over a large field range, from 0.1 to 11.7 T. The shape of the curve for R_1 as a function of field and a model-free analysis were used to extract τ_c, a correlation time for each type of phospholipid molecule in the bilayer that is likely to reflect rotation of the molecule about the axis perpendicular to the membrane surface; S_c^2, a chemical shift anisotropy (CSA) order parameter; and τ_{hf}, a time constant reflecting faster internal motion. This ^{31}P technique was also used to monitor association of a peripheral membrane protein, *Bacillus thuringiensis* phosphatidylinositol-specific phospholipase C, with both phosphatidylcholine and phosphatidylmethanol bilayers. Differences in phospholipid dynamics induced by the protein shed light on how zwitterionic phosphatidylcholine, and not the anionic phosphatidylmethanol, activates the enzyme toward its substrate.

^{31}P NMR spectroscopy was an early tool for characterization of phospholipid bilayer structure. For large multilamellar structures, the line shape reflected the particle morphology (lamellar, hexagonal, isotropic; for reviews, see refs 1−3), and changes in the powder-pattern line width served as a way of monitoring phase transitions (e.g., from gel to liquid-crystalline phase). For small vesicles, chemical shift differences of ^{31}P resonances for two populations of a phospholipid in slow exchange (most often induced with the addition of paramagnetic ions) have been used to determine the distribution of phospholipid components on each leaflet of the vesicle.[4] Detectable {^{1}H−^{31}P} NOEs for these particles at low field were used to show qualitatively the dynamic nature of molecules[5] and, in particular, to suggest interactions between the methyl tails of the acyl chains and the phosphorus group of phosphatidylcholine.[6] Furthermore, changes in line width (or chemical shift) have been used to indicate interactions of phospholipids with other components (cholesterol, other lipids, peptides, proteins; for examples, see refs 2, 7, and 8) added to the membrane.

^{31}P T_1 values as well as line width changes have been measured for phospholipid molecules in different aggregates.[2,9]

In principle, these measurements should provide a detailed description of phospholipid dynamics. However, interpretation of these relaxation rates is difficult in the case of vesicles (and in general any ^{31}P that has no attached ^{1}H) at the moderate to high fields needed to distinguish multiple phospholipid components, since both chemical shift anisotropy as well as dipolar interactions can contribute to the relaxation rate. Typically, researchers have looked for minima in the temperature dependence of T_1 for comparative purposes.[2] For phospholipid small unilamellar vesicles (SUVs), measured relaxation rates do not reflect vesicle tumbling, but rather provide information on faster local motions (e.g., rotation about the long molecular axis of a phospholipid molecule, segmental motions of the phospholipid headgroup, lateral diffusion, collective motions in the plane of the bilayer), although the contribution of these motions to T_1 is a matter of some dispute. Proton field-cycling studies[10−12] over a very broad frequency range are consistent with diffusional processes (but not individual segment dynamics) dominating relaxation in the MHz range. The large size of the vesicles causes spin diffusion among proton spins and complicates interpretation of ^{1}H−^{31}P NOE experiments.[6] ^{31}P relaxation is likely to be dominated by chemical shift anisotropy (CSA) and not dipolar interactions at higher fields. Clearly, there is a wealth of quantitative information (the very least of which are correlation times) in the relaxation rates, but difficulty in extracting it.

High-resolution field-cycling NMR spectroscopy is a novel technique that can measure spin−lattice relaxation rates ($R_1 = 1/T_1$) of samples with multiple resonances over a large field

† Boston College.
‡ Brandeis University.
(1) Seelig, J. *Biochim. Biophys. Acta* **1978**, *515*, 105−140.
(2) Smith, I. C. P.; Ekiel, I. H. In *Phosphorus-31 NMR: Principles and Applications*; Gorenstein, D. G., Ed.; Academic Press: Orlando, FL, 1984; pp 447−475.
(3) Fenske, D. B.; Cullis, P. R. *Encyclopedia of NMR*; Grant, D. M., Ed.; Wiley & Sons: New York, 1995; pp 2730−2735.
(4) Grasdalen, H.; Goran Eriksson, L. E.; Westman, J.; Ehrenberg A. *Biochim. Biophys. Acta* **1977**, *469*, 151−162.
(5) Tauskela, J. S.; Thompson, M. *Biochim. Biophys. Acta* **1992**, *1104*, 137−146.
(6) Yeagle, P. L.; Hutton, W. C.; Huang, C.; Martin, R. B. *Proc. Natl. Acad. Sci. U.S.A.* **1975**, *72*, 3477−3481.
(7) Swairjo, M. A.; Seaton, B. A.; Roberts, M. F. *Biochim. Biophys. Acta* **1994**, *1191*, 354−361.
(8) Pinheiro, T. J.; Duer, M. J.; Watts, A. *Solid-State NMR* **1997**, *8*, 55−64.

(9) Fenske, D. B. *Chem. Phys. Lipids* **1993**, *64*, 143−162.
(10) Rommel, E.; Noack, F.; Meier, P.; Kothe, G. *J. Phys. Chem.* **1988**, *92*, 2981−2987.
(11) Kimmich, R.; Voigt, G. *Chem. Phys. Lett.* **1979**, *62*, 181−183.
(12) Kimmich, R.; Schnur, G.; Scheuermann, A. *Chem. Phys. Lipids* **1983**, *32*, 271−322.

range, from nearly zero to 11.7 T, in our case using a commercial high-resolution instrument for preparation and readout.[13,14] The method is particularly useful for nuclei such as ^{31}P without directly attached protons, e.g., in biological phosphate esters, where the relatively large CSA complicates extracting correlation times from relaxation rates using fixed-field NMR. Our shuttling system, designed for simple construction and easy installation in a Varian INOVA[plus] instrument, carries the sample pneumatically from the probe to a point in the fringe field in about 0.1−0.3 s, and then back into the probe, for analysis of the response of individual resonances to the lower field environment. We have previously used it for accurate measurement of [1]H R_1 up to ∼20 s^{−1} ($T_1 \approx 50$ ms) and [31]P R_1 up to ∼5 s^{−1} for a DNA octamer duplex.[14] This report, like the study of the DNA, is intended to show the applicability of these techniques for the study of phospholipid membranes. It differs from the previous report on the DNA octamer in that we study a large variety of phospholipid samples, and that, because the membrane systems are more complicated, we are not able to present such a complete theoretical explanation of our observations. However, the results presented clearly indicate that high-resolution ^{31}P field-cycling is a novel and information-rich way to monitor vesicle dynamics. The reader may wish to look at the previous article on the DNA octamer[14] while reading this one, since we use some of the same language and interpretation.

Materials and Methods

Vesicle Preparation. Lipid (1-palmitoyl-2-oleoyl-phosphatidylcholine (POPC), dioleoylphosphatidylmethanol (DOPMe),1-palmitoyl-2-oleoyl-phosphatidic acid (POPA), phosphatidylinositol (PI), and diheptanoylphosphatidylcholine (diC$_7$PC)) stock solutions in chloroform were obtained from Avanti Polar Lipids (Alabaster, AL) and used without further purification. After removal of the chloroform with a stream of N$_2$, the lipid film was lyophilized and then rehydrated with buffer containing 25−95% D$_2$O (99.9%, Sigma-Aldrich, Saint Louis, MO), depending on the particular sample and whether ^{1}H field-cycling experiments were to be carried out. For ^{31}P-only work, the buffer used was 50 mM MES, 1−5 mM EDTA (with the higher concentration used with anionic phospholipids), pH 7.5; when ^{1}H cycling was also to be examined, the phospholipids were rehydrated in 20 mM borate buffer, pH 7.5, or imidazole (pH 7.0) made with 99.9% D$_2$O. A polymerizable phosphatidylcholine, 2,3-bis[12-(lipoyloxy)dodecanoyl]-sn-glycero-1-phosphocholine (BLPC), obtained from Dr. Wonhwa Cho, University of Illinois Chicago Circle, was also used to form small vesicles.[15] SUVs were prepared from these different suspensions by sonication using a Branson sonifier cell disrupter until maximum clarity was achieved (typically 5−10 min). The typical preparation had an average vesicle diameter of 250−300 Å (as estimated by light scattering). In the case of the polymerizable PC, the vesicle solution was agitated vigorously after a small amount of dithiothreitol (Bio-Rad, Hercules, CA) was added to initiate cross-linking of the protected terminal thiols.[15] Large unilamellar vesicles (LUVs) were prepared by multiple passages of the unsonicated aqueous lipid solutions through polycarbonate membranes (100-nm pore diameter) using a Lipofast extruder from Avestin (Ontario, Canada). Bicelles were prepared by mixing a suspension of dipalmitoylphosphatidylcholine (DPPC) multilamellar vesicles with micellar diC$_7$PC, then heating the sample above the gel to liquid crystalline phase transition of the long-chain component, and then cooling to room temperature. Under these conditions, it has previously been shown that a relatively uniform population of 200−250 Å diameter particles is formed at room temperature.[16]

PI−PLC. Overexpression and purification of recombinant *Bacillus thuringiensis* PI-specific phospholipase C (PI−PLC) was carried out as described previously.[17] Protein solutions were concentrated using Millipore Centriplus 10 filters (Billerica, MA); concentrations were estimated by A$_{280}$ using the extinction coefficient calculated from the protein sequence. For vesicle samples (0.3 mL in 5-mm NMR tubes), the enzyme was mixed with an aliquot of an SUV stock solution to yield 6 mg/mL PI−PLC and 15 mM phospholipids, either POPC or DOPMe in the MES buffer.

NMR Methods. [31]P and [1]H T_1 and T_2 measurements were made at 11.74 T on a Varian INOVA 500 using standard inversion−recovery and Carr-Purcell-Meiboom-Gill sequences. The nonselective field-cycling [31]P R_1 experiments (for details on pulse sequence, see ref 14) were run at 22 or 30 °C on the same Varian Unity[plus] spectrometer using a standard 10-mm Varian probe and modified slightly for high-resolution field cycling, as described previously.[13,14] Vesicle samples were sealed as described[13] in 5-mm tubes, or in a few cases 8-mm NMR tubes, with bulk phospholipid concentrations of 5−30 mM of each phospholipid depending on vesicle and sample tube size. The larger 8-mm NMR tubes would have been desirable, but components for them were not always available, and expediency led us to use the smaller 5-mm tubes. Initially, samples were purged with helium gas before sealing in the NMR tubes. However, this was later found to be unnecessary for the vesicle samples. Relaxation experiments at a given field strength were typically 1−5 h (depending on sample concentration and field), each with 6−8 programmed delay times. Proton R_1 rates were measured (with fewer transients) in a nonselective manner using the same nonselective field-cycling methods as for [31]P.

Data Analysis and Relaxation Theory, [31]P. We present here simply the mathematical expressions used (suggested by the model-free approach[18,19]) to fit the data[14] and discuss their physical interpretation in the next section. The field dependence of R_1 from field cycling was analyzed in terms of three field-dependent contributions to R_1:

$$R_1 = [R(0)/2\tau_c][0.1J(\omega_H - \omega_P) + 0.3J(\omega_P) + 0.6J(\omega_H + \omega_P)] + C_L\omega_P^2 J(\omega_P) + C_H H^2 \quad (1)$$

Here, $R(0)$ is the dipolar relaxation rate associated with τ_c at zero field; ω_P and ω_H are the angular frequencies of the phosphorus and proton, equal to their gyromagnetic ratios multiplied by the field; $J(\omega)$ equals $2\tau_c/(1 + \omega^2\tau_c^2)$; and H is the field in Tesla. The last two terms in eq 1 reflect low-frequency and high-frequency contributions of the CSA interaction to relaxation.[14] Along with the raw fitting parameters C_L and C_H, we extract an order parameter S_c^2 and a high-frequency correlation time τ_{hf}. These are defined in terms of the raw fitting parameters C_L and C_H by

$$C_L = (1/15)(1 + \eta^2/3)\sigma^2 S_c^2 \quad (2)$$

and

$$C_H = (2/15)\gamma_P^2(1 + \eta^2/3)\sigma^2(1 - S_c^2)\tau_{hf} \quad (3)$$

Here γ_P is the gyromagnetic ratio, and σ and η define the CSA interaction size and asymmetry. We assumed values for them of 160 ppm and 0.57, respectively, as previously determined for DPPC in 50 wt % water at 163 K.[20]

The parameter $R(0)$, which is the relaxation time in the apparent zero field limit, is extracted directly from the data and often used directly in our discussion. It is a useful parameter because it varies strongly

(13) Redfield, A. G. *Magn. Reson. Chem.* **2003**, *41*, 753−768.
(14) Roberts, M. F.; Cui, Q.; Turner, C. J.; Case, D. A.; Redfield, A. G. *Biochemistry* **2004**, *43*, 3637−3650.
(15) Wu, S.-K.; Cho, W. *Biochemistry* **1993**, *32*, 13902−13908.

(16) Gabriel, N. E.; Roberts, M. F. *Biochemistry* **1986**, *25*, 2812−2821.
(17) Feng, J.; Webhi, H.; Roberts, M. F. *J. Biol. Chem.* **2002**, *277*, 19867−19875.
(18) Szabo, A. *Ann. N.Y. Acad. Sci.* **1986**, *482*, 44−50.
(19) Lipari G.; Szabo, A. *J. Am. Chem. Soc.* **1982**, *104*, 4546−4559.
(20) Herzfeld, J.; Griffin, R. G.; Haberkorn, R. A. *Biochemistry* **1978**, *17*, 2711−2718.

between different samples. However, in place of $R(0)$ it is sometimes of interest to use instead another parameter, r_{eff}, which may represent the effective distance between the phosphorus and proton(s) responsible for the dipolar relaxation. The parameter r_{eff} is defined in terms of the correlation time τ_c and the zero-field relaxation rate $R(0)$ by the equation

$$R(0) = \tau_c (\mu_o/4\pi)^2 (h/2\pi)^2 \gamma_P{}^2 \gamma_H{}^2 r_{eff}{}^{-6} \qquad (4)$$

where h is Planck's constant, μ_o is the permittivity of free space, and γ_P and γ_H are the phosphorus and proton gyromagnetic ratios, respectively.

Thus, in sum, we ultimately fit the field-dependent data with four parameters τ_c, $S_c{}^2$, τ_{hf}, and either $R(0)$ or r_{eff}. This analysis is convenient, even though it does not properly account for the highly anisotropic diffusion of the phospholipids. It provides a simple phenomenological description of the behavior of the different samples and conditions that we used.

Relaxation Theory for Strongly Anisotropic Diffusion. The theory for this problem is described below without great detail, since we did not attempt to fit the data to this theory. Such a fit is problematic because some parameters that are needed are unknown and because the fitting procedure described above provides an adequate characterization of our data. However, the brief description here is intended to support our later discussion about interpretation of the parameters that we tabulated.

We predicted dipolar relaxation from the theory provided by Woessner[21,22] for a disk-shaped molecule, taking his internal correlation time to be the inverse of the rotational diffusion constant about the director in our case, and taking the other molecular diffusion rates to be zero. As indicated below, it is likely that this motion is the major relaxation mechanism for ^{31}P in these membranes above 0.1 T, other than the high-frequency motion that is fit by the last term of eq 1. The resulting prediction has six terms and depends on the angle, Δ, between the phosphorus−proton vectors and the membrane director. If on average Δ is between about 30 and 90°, as is likely, the theory is dominated by terms identical in form to the first three terms in brackets in eq 1. The parameter τ_c is the inverse of the angular rotational diffusion constant of the phospholipids about the director. Equation 4 above is modified, being multiplied by a factor of $3(\sin 2\Delta)^2/4$, provided $30° < \Delta < 90°$.

Expressions for the CSA contribution to relaxation for anisotropic rotational diffusion have been given by Kowalewski and Werbelow.[23] To apply these results to our problem we made the same assumption about the rotational diffusion coefficients described in the last paragraph. The relaxation rate is predicted to be highly dependent on the orientation of the CSA tensor with respect to the membrane director. For the special cases where one of the three CSA principal axes is along the director, eq 10 from Kowalewski and Werbelow[23] applies and predicts that the rate is proportional to the square of the difference between the CSA tensor principal values along the two axes other than the one that is along the director. Of the three CSA orientations of this special type, the rate is thus predicted to be smallest when the director is along the direction of the largest CSA tensor element, and largest when it is along the direction of the tensor element having the smallest absolute value. The CSA tensor principal values deduced from the reported[29] values of σ and η, 160 ppm and 0.57, are +106, −18, and −78 ppm. The smallest and largest rates predicted from these values are, respectively, 0.34 and 4.1, times the value predicted by the next-to-last term of eq 1 with the same rotational correlation time and order parameter $S_c{}^2 = 1$, which is appropriate for isotropic rotational diffusion with no internal motion. These rates do not take into account any possible asymmetry of the CSA tensor, which is likely to be small,[23] and are likely to be

(21) Woessner, D. E. *J. Chem. Phys.* **1962**, *37*, 647−654.
(22) Woessner, D. E. In *Encyclopedia of NMR*; Grant, D. M., Ed.; Wiley & Sons: New York, 1995; pp 1068−1083.
(23) Kowalewski, J.; Werbelow, L. *J. Magn. Reson.* **1997**, *128*, 141−148.

the minimum and maximum values of the predicted rates for any orientation of the CSA tensor. However, since we do not know the orientation of the CSA axis with respect to the director, we did not attempt to calculate a more exact expression for the high-field CSA relaxation contribution (last term of eqs 1 and 3).

Data Analysis, Protons. The field dependence of ^{1}H resonances could not be fit by simple dipolar relaxation, but could be well fit with a field-dependent term approximating dipolar relaxation with a single correlation time scale $\tau_H{}^2$ and a field-independent term c, which is probably the contribution of spin-diffusion-mediated homonuclear dipolar relaxation by fast internal motion:

$$R_1 = R(0)/(1 + \gamma_H{}^2 H^2 \tau_H{}^2) + c \qquad (5)$$

This simplistic expression will allow us to compare τ_H (which will vary significantly depending on the proton in the molecule and the extent of segmental motion) to the τ_c extracted from the ^{31}P field-cycling data.

Results and Discussion

^{31}P Relaxation in Vesicles. We first present the data for a well-behaved binary vesicle system of 1-pamitoyl-2-oleoyl-phosphatidylcholine and dioleoylphosphatidylmethanol (POPC/DOPMe) and the values of the phenomenological parameters mentioned in the Experimental Section that are used to fit and describe these data. Then after a brief review of the "model-free" formalism[18,19] applied to the case of spherical macromolecules, we discuss the likely interpretation of its parameters in terms of dynamic and structural properties of phospholipids in membranes. We then provide a brief interpretation of the POPC/DOPMe data. Following this, we will provide three sections describing experiments on different but related phospholipid aggregates that were designed to test and clarify our conjectures. The end of this section has a discussion of possible corrections to these parameters that would result if a complete theory could be applied with more information. We also consider what quantitative conclusions we can make about phospholipid structure and dynamics from these results.

POPC/DOPMe SUVs. Data. SUVs, with a diameter in the range of 250−300 Å, were formed with a 1:1 mixture of zwitterionic POPC and anionic DOPMe. At 22 °C, both components in membrane vesicles are well above the melting transition for each pure lipid and should be well-mixed in the bilayer. As shown in Figure 1A, ^{31}P spectra clearly show well-separated resonances for the two species of moderate line width ($\sim$60−75 Hz). The field dependence of the ^{31}P relaxation rate (R_1) for each phospholipid in this two-component system is shown in Figure 2A. There are three distinct regions in the curve, superficially similar to what we have seen in DNA.[14] (i) Below 1 T, the relaxation rate increases as the field decreases; (ii) around 1−2 T, R_1 reaches a minimum and begins to increase; and then (iii) above 4 T, R_1 increases with a square law dependence. It is the intermediate- to high-field region that has been sampled in previous fixed field[6] and limited variable field[24] ^{31}P studies of vesicles in attempts to characterize phospholipid dynamics in bilayers. With eq 1, the curves can be decomposed phenomenologically (as done previously for DNA[14]) into the three relaxation components: dipolar, CSA, and high-field CSA (see Figure 2B for this deconvolution in the case of DOPMe). Both POPC and DOPMe motions are characterized by the same correlation time, $\tau_c \approx 5$ ns, and an $R(0)$ around 1 s^{-1}; however,

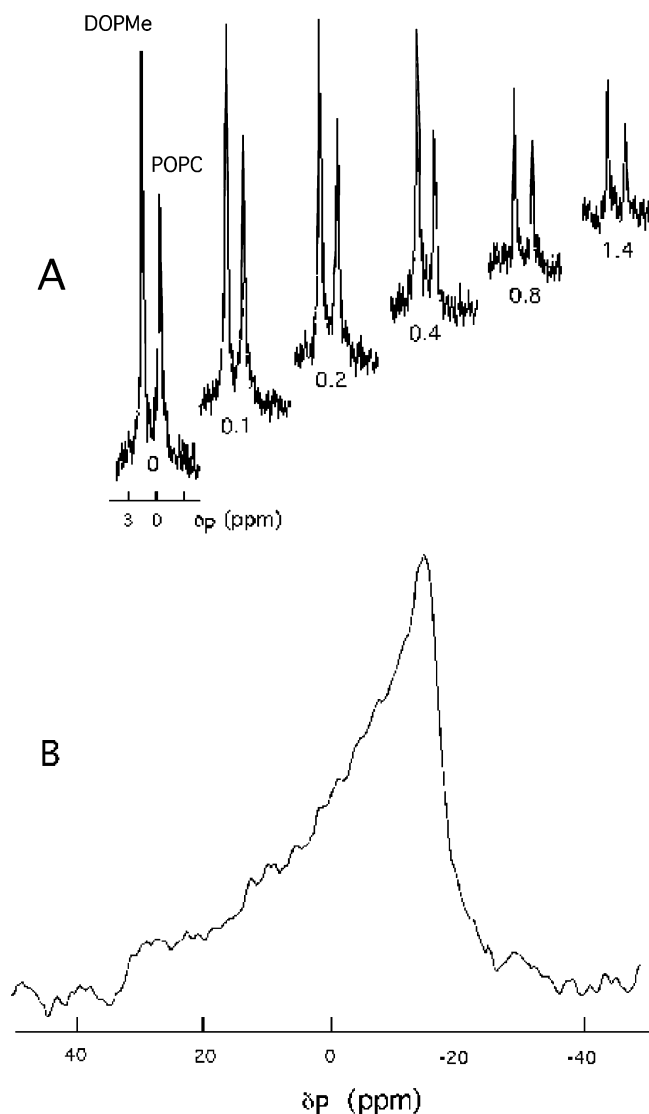(24) Milburn, M. P.; Jeffrey, K. R. *Biophys. J.* **1987**, *52*, 791−799.

Figure 1. (A) ^{31}P spectra from a field-cycling T_1 experiment at 0.14 T for POPC(30 mM)/DOPMe (30 mM) SUVs sealed in a 5-mm NMR tube in 50 mM MES, pH 7.5 (the relaxation delay time in seconds spent at 0.14 T is indicated beneath each spectrum). (B) ^{31}P spectrum (11.74 T) of cross-linked BLPC SUVs (10 mM) in the same buffer.

Figure 2. (A) [31]P R_1 as function of magnetic field for SUVs composed of 30 mM POPC (■) and 30 mM DOPMe (●). (B) Deconvolution of the DOPMe [31]P R_1 dependence into dipolar (—), CSA (− − −), and high-field CSA (···) components.

the CSA terms are different for the two phospholipids. The parameters extracted from this analysis are given in Table 1.

Interpretation of Correlation Times. Our gross interpretation of these data is that the rise in R_1 below about 2 T is due to magnetic dipolar interaction between the phosphorus spins and nearby protons, while relaxation at higher field is due to the chemical shift anisotropy. Both of these interactions could be treated by the model-free formalism,[18,19] which is widely applied to macromolecules free in solution. For a nearly spherical molecule, such as the small DNA duplex we worked on previously,[14] equations such as those in the last sections would apply, with τ_c being the overall rotational correlation time of the molecule, S_c^2 being an order parameter for the partial averaging of the CSA interaction by internal high-frequency dynamics, and τ_{hf} being the time scale of these internal motions. The parameter r_{eff} is a measure of the distance of nearby protons. For a rigid macromolecule, r_{eff} would be the inverse sixth root of the sum $\Sigma(r^{-6})$ for all protons surrounding the phosphorus, where r is the distance from each proton to the phosphorus. In
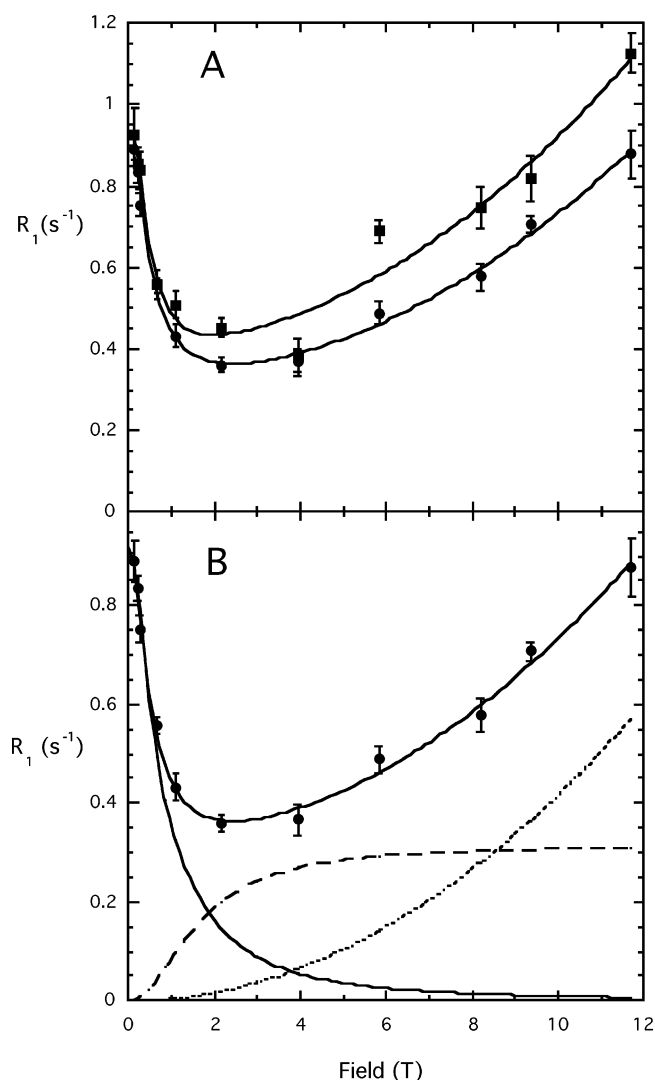
most cases, including the present one, this parameter, as deduced from the observed value of $R(0)$, would be decreased by the sixth root of a *dipolar* order parameter S_d^2, which we omitted as a multiplier on the right side of eq 5 above. We avoid use of this order parameter because we have no way to determine it separately from r_{eff} using our data. This means that the values of r_{eff} that we deduce for POPC and DOPMe (2.80 and 2.83 Å, respectively) may not provide a true value for the phospholipid geometry if the relevant dipolar order parameter S_d^2 differs very much from one. If $S_d^2 < 1$, then the true r_{eff} sum will be somewhat less than what we extract from this analysis.

As to the interpretation of the time-scale parameters τ_c and τ_{hf} in the present case, the longest time scale expected to be felt by the phospholipid is from the change in orientation of its major axis parallel to the membrane director. This time scale is the inverse of the sum of the rates for overall rotation of the vesicle, plus the rate for lateral diffusion of an individual phospholipid molecule from one side of the vesicle to the other, plus the rate for flip-flop of the phospholipids from the inner to the outer leaflet of the vesicle. The last rate is expected to be negligible. The first two rates for these small vesicles should

Table 1. Relaxation Parameters, $R(0)$, τ_c, C_L, C_H, S_c^2, and r_{eff}, for Phospholipid Components of SUVs Extracted from ^{31}P Field-Cycling Experiments[a]

sample	$R(0)$ (s^{-1})	r_{eff} (Å)[b]	τ_c (ns)	$C_L \times 10^8$	$S_c^{2\ c}$	C_H	τ_{hf} (ps)[d]
DOPMe/POPC:							
DOPMe	0.92 ± 0.03	2.83	5.1 ± 0.5	0.16 ± 0.02	0.42	0.0038 ± 0.0003	140
POPC	0.96 ± 0.07	2.80	5.0 ± 1.4	0.18 ± 0.06	0.46	0.0055 ± 0.0007	220
+ cholesterol:							
DOPMe	1.30 ± 0.40	3.00	9.3 ± 1.5	0.36 ± 0.10	0.93	0.0047 ± 0.0010	–
POPC	1.50 ± 0.60	2.80	11.6 ± 1.4	0.57 ± 0.11	1	0.0046 ± 0.0008	–
BLPC (30 °C):	2.58		7.5 ± 2.3	0.35 ± 0.21	0.89	0.0059 ± 0.0019	–
POPA/POPC							
(22 °C):							
POPA	1.14 ± 0.29	2.81	6.1 ± 3.8	0.23 ± 0.17	0.60	0.0023 ± 0.0005	130
POPC	1.63 ± 0.14	2.87	9.7 ± 3.2	0.55 ± 0.21	1	0.0036 ± 0.0011	–
(30 °C):							
POPA − out	1.27 ± 0.12	2.93	8.7 ± 1.9	0.29 ± 0.08	0.76	0.0028 ± 0.0004	250
POPA − in	1.75 ± 0.50	2.88	11.5 ± 7.5	0.38 ± 0.09	0.97	0.0044 ± 0.0008	–
POPC	0.99 ± 0.10	2.86	5.8 ± 1.7	0.25 ± 0.08	0.64	0.0063 ± 0.0006	380
LUVs	1.41	2.84	7.9	0.26	0.67	0.0045	300
PI/PC	1.72 ± 0.13	2.59	5.6 ± 1.5	0.25 ± 0.10	0.65	0.0044 ± 0.0012	270
diC$_7$PC/DPPC							
(1:4)	1.52 ± 0.20	3.37	16.3 ± 4.3	0.57 ± 0.15	$-^e$	0.0057 ± 0.0002	–
(1:2)	1.03 ± 0.09	2.91	9.9 ± 3.8	0.42 ± 0.24	$-^e$	0.0038 ± 0.0014	–

[a] Field cycling carried out at 22 °C unless otherwise indicated. [b] Uncertainties in r_{eff} are <0.05 Å because r_{eff} is proportional to $R(0)^{-6}$. [c] Uncertainties in S_c^2 values within the model we used to extract these from C_L are <40% (and usually under 30%) except for the cross-linked SUVs and POPA at 22 °C. [d] Since evaluation of τ_{hf} depends on S_c^2, there is likely to be considerable uncertainty in this parameter, and therefore only two significant figures are shown. [e] The S_c^2 extrapolated from C_L is greater than one, making it impossible to interpret C_H.

be in the range of 10^6 s^{-1} estimated for a 200–300 Å diameter spherical vesicle.

Clearly, the motional time scale τ_c reported by the low-field dipolar part of the relaxation curve is not the time scale of lateral diffusion or overall vesicle tumbling, since our experimental values for τ_c are in the nanosecond range, rather than the microsecond range expected. The relaxation observed at these low fields must be due to the ^{31}P-to-proton dipolar interaction, since CSA relaxation should become negligible at low field and there are no other reasonable mechanisms. This time scale is almost certainly due to rotational diffusion (averaged over the subnanosecond time scale of any internal motion) of the vectors connecting the phosphorus nucleus to the nearest glycerol (*sn*-3) protons, since this motion produces a large modulation of the phosphorus–proton dipolar interaction unless these vectors happen to be pointing along or nearly along the membrane director. Vesicles made in 95% D$_2$O as well as in 25% D$_2$O showed no appreciable difference in the R_1 versus field profile consistent with little relaxation by water in this system. For a variety of reasons (distance, polar side-chain flexibility), we assume that other nearby protons would not be likely to contribute much to this relaxation in most cases (vide infra). The R_1 that we measure experimentally would, of course, be the sum of the rates due to each of these two glycerol protons, which we assume to be similar in magnitude.

Thus, our working hypothesis is that the correlation time τ_c, which we use to fit the low-frequency relaxation, is the next-slowest time scale after lateral diffusion and vesicle tumbling that we can imagine for the phospholipids. Thus, τ_c could report relative diffusion time of the alkyl chains around each other, about the molecular axis (the membrane director). Such a time scale for ^{31}P-group motion does not seem to have been explicitly considered in recently published presentations of computer simulations of phospholipid motion. However, the relative motion of the vector connecting two carbons, each in the middle

of the two different alkyl chains of a PC molecule in a bilayer, was found to have a time scale similar to our τ_c.[25]

Other motions, possibly of the glycerol backbone, could also contribute to the 5-ns τ_c we measure for both phosphates of POPC/DOPMe SUVs. In considering these possibilities, the amplitudes of potentially important motions should be considered carefully. Motions that are hindered by covalent or other features of the structure to allow less than 360° rotation are likely to be less efficient than those that result in complete rotation, such as the rotational diffusion of the phospholipids about the director.

The shorter time scales described by the tabulated values τ_{hf} are not as well-determined because they are inferred very indirectly and are based, to a greater extent, on theory rather than being deduced, like τ_c, largely from the inverse of the angular frequency of a feature of the plot of R_1. We assume that τ_{hf} reflects the rate for motion among several relatively stable positions of the headgroup that are allowed by the orientation of the time-averaged glycerol backbone orientation. However, a problem with this speculation is that there may not be well-separated groups of correlation times as is assumed for protein applications of the model-free theory.

Therefore, in contrast to our previous field-cycling study of DNA, our tabulated values of τ_{hf} are useful only as rough and tentative indicators because the parameter C_L cannot be estimated experimentally well enough to give an order parameter S_c^2 that is statistically different from one, and, more importantly, the relaxation time predicted by the more exact theory described in the Methods section depends strongly on the orientation of the CSA tensor relative to the membrane director.

Interpretation of POPC/DOPMe SUV Parameters. The S_c^2 and τ_{hf} parameters estimated from C_L and C_H for this sample (Table 1) suggest that the phosphates of each of the two

(25) Moore, P. B.; Lopez, C. F.; Klein, M. L. *Biophys. J.* **2001**, *81*, 2484–2494.
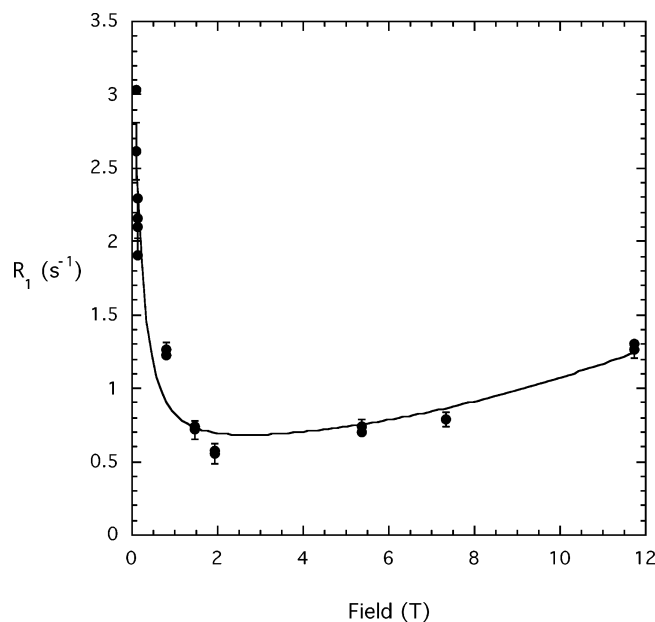
Figure 3. Field dependence of R_1 for SUVs composed of cross-linked BLPG (10 mM) at 30 °C.

Figure 4. Effect of 33 mol % cholesterol (20 mM) on the field dependence of ^{31}P R_1 for SUVs containing 20 mM DOPMe (■, □) and 20 mM POPC (●, ○). The open symbols reflect R_1 for each lipid in the presence of cholesterol. Lines (solid for without and dotted with cholesterol) are the best fits to eq 1. The semilog plot emphasizes the increase in $R(0)$ in the presence of cholesterol.

components exhibit similar CSA ordering as well as τ_c in this fluid bilayer. However, internal motion for the POPC phosphate appears slower ($\tau_{hf} = 220$ ps) than that of DOPMe ($\tau_{hf} = 140$ ps). This difference in τ_{hf} for the two phospholipids is based on a statistically significant difference in C_H for the two phospholipids. Interestingly, the values for τ_{hf} are similar to τ_{hf} values for the phosphorus nuclei in a DNA octamer obtained by field cycling.[14] The similarity in $R(0)$ also indicates nearly identical r_{eff} for both phospholipid components in these SUVs.

Motions Reflected in τ_c: Cross-Linked PC SUVs and Effects of Cholesterol. As mentioned, τ_c could represent rotation of the entire phospholipid molecule around its long axis perpendicular to the membrane surface, and/or it could reflect glycerol torsional motions that alter the position of the phosphate. It was pointed out above that τ_c is a definite time scale extracted almost directly from the width of the low-field rise in the relaxation rate, whereas the values extracted for τ_{hf} rely on the model-free analysis.

To test the hypothesis that τ_c reflects molecular rotation about the director, polymerized vesicles composed of BLPC[15] were examined by ^{31}P field cycling. BLPC molecules are cross-linked at the ends of the acyl chains and likely to range in size from dimers to ~8−10 cross-linked molecules. Although the vesicles were small (<300 Å average diameter since the sample was nearly optically clear), the ^{31}P spectrum obtained at 30 °C appeared to be a standard powder pattern for axial CSA with slow rotation (Figure 1B).

The field dependence of the cross-linked BLPC vesicles (Figure 3) exhibited a relaxation pattern similar to that for uncross-linked SUVs with a τ_c of 7.5 ± 2.3 ns if the intensity of the high-field sharp edge of the spectrum was monitored (~10 ns if the area under the curve is monitored). Complete rotation of an individual phospholipid molecule should be dramatically hindered by cross-linking the tails of several molecules together. The rotation rate, $1/\tau_c$, while high, was still in the range seen for other SUV systems (Table 1). Thus, rotation of an individual molecule around an axis perpendicular to the vesicle surface may not be the only contributor to this time scale motion,
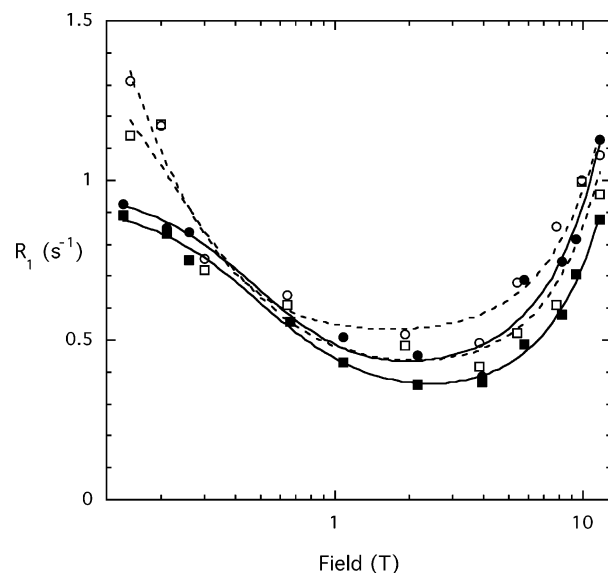
although it is possible that our observation reflects the wide range of degree of polymerization of the phospholipids with, perhaps, dimers and trimers dominating the observation. The latter could more or less dominate the spectrum and relaxation. However, it has been found in simulations that torsional motions of the headgroup, and notably those involving glycerol backbones, are very slow and in the nanosecond range.[26] These types of isomerizations (as well as glycerol crankshaft-type motions[27]) coupled to acyl chain reorientations could also contribute to τ_c. For the cross-linked PC, these motions rather than molecular rotation, could provide the major relaxation pathways.

In fact, we do not understand the spectrum (Figure 1B) of this cross-linked molecule very well. The rotational correlation time for a 300 Å diameter vesicle should be about 10 μs, if transverse diffusion is assumed to be prevented by the cross-links. But the spectrum of Figure 1B has features that appear broadened by about 1000 Hz. If this is simple lifetime broadening, the deduced lifetime is about 300 μs, much longer than the expected correlation time. It is possible that heterogeneity of the sample produces only superficial resemblance to a classic powder pattern.

Cholesterol added to the bilayer should also dramatically slow such isomerizations, and, indeed, POPC/DOPMe SUVs with 30% cholesterol exhibited dramatically altered R_1 versus field profiles (Figure 4). Simply examining the data plotted as R_1 versus log(field), we see that the $R(0)$ value has increased, consistent with an increased τ_c. R_1 in the mid-field region (2−7 T) is clearly also shifted to higher values. If the only change were an increased τ_c, R_1 should decrease in the mid-field region since the limit for R_1(CSA) is proportional to $1/\tau_c$. An upward shift in the curve indicates that S_c^2 has increased for both phospholipids along with the longer τ_c indicated by the increased

(26) Pastor, R. W.; Venable, R. M.; Feller, S. E. *Acc. Chem. Res.* **2002**, *35*, 438−446.
(27) Strenk, L. M.; Westerman, P. W.; Doane, J. W. *Biophys. J.* **1985**, *48*, 765−773.

$R(0)$. The extracted averaged distance r_{eff} is 2.9 ± 0.1 Å for the two phospholipids with cholesterol, a value within error of r_{eff} in the absence of cholesterol. Since S_c^2 has increased and is near 1, the errors in estimating τ_{hf} from C_H are large. However, the model-free formalism would suggest that this motion is significantly dampened ($\tau_{hf} \geq 0.5$ ns) by the inclusion of cholesterol in the vesicle. Clearly, the field dependence of ³¹P relaxation for both phospholipids in the SUVs is sensitive to motions of the phospholipid chains as well as local ordering, by either chemically cross-linking the tails or adding cholesterol.

Corrections Arising from the Use of Theory of Relaxation with Anisotropic Motion. The nanosecond-range parameter τ_c obtained from our fitting surely measures some real dynamic process in the molecule, because it was determined from frequencies of spectral features alone, in the variation of relaxation rate versus frequency. The theory that is applicable to the present problem is discussed at the end of the Methods section. Unless the angle between the phosphorus and the relevant (probably glycerol *sn*-3) protons and the membrane director is less than 20° or between 80 and 90°, the theory shows that the value of τ_c that we report is close to the inverse of the angular rotational diffusion constant (in rad²/s) for rotation of the phospholipids about the director axis. Errors introduced by the fact that our fitting procedure is more appropriate for isotropic rotational diffusion and by the more complicated frequency dependence of the anisotropic theory are likely to produce only a small error in τ_c.

The true value of the geometric parameter r_{eff} that we infer and list in Table 1 could be smaller than the values tabulated, as a result of our omission of a dipolar order parameter multiplying the right side of eq 4. This could result from a large-magnitude high-frequency motion. Dipolar order parameters in the range of 0.5 to 0.8 are often inferred for isolated amide NH groups in proteins.

An error in the same direction is indicated by the exact dipolar relaxation theory. The expression for $R(0)$ is also theoretically decreased by a factor that depends on the angle between the P to proton vector and the director. We have recently been able to estimate this angle by observations at fields below 0.05 T (to be reported when complete and analyzed) and expect that this correction is about 0.25 for $R(0)$ in those cases that we have studied.

The time-scale parameter τ_{hf} was estimated rather indirectly from eqs 2 and 3. Because the estimate of τ_{hf} is based on a difference between estimates from experiments at an intermediate field and a theoretical value that differs from the value used in eq 1 by a factor of as much as 3, the tabulated values of this time scale and of S_c^2 are useful mainly as rough indicators of the true time scale. The wide range of the τ_{hf} values and the fact that the inferred values of S_c^2 in Table 1 are often very close to 1 suggest that the tabulated order parameters and τ_{hf} values are for the most part too high compared to their true values. The data do indicate the existence of high-frequency motion, but the time scale may be several times faster than indicated by the fitted values.

POPA/POPC Vesicles. Protons Responsible for Phosphorus Relaxation. Phosphatidic acid lacks any alcohol esterified to the phosphate (it has no side chain), and field cycling of vesicles with this phospholipid will allow us to test the importance of the polar group for both τ_c and τ_{hf} motions. With
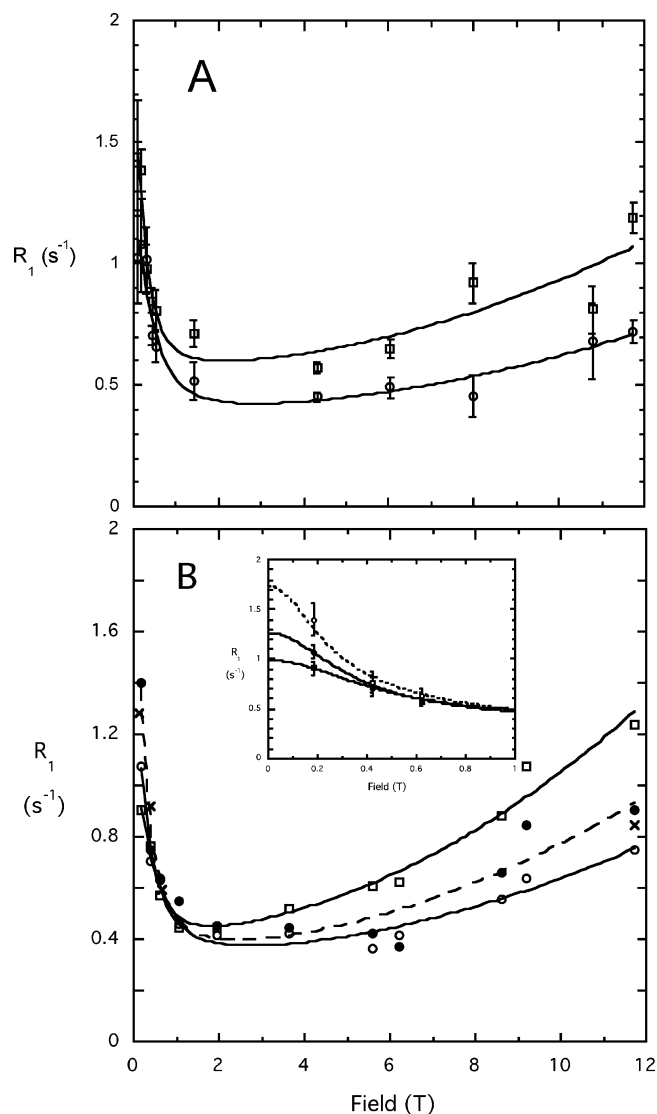

Figure 5. Field dependence of ³¹P R_1 for POPC/POPA SUVs (A) at 22 °C and (B) 30 °C: □, POPC; ○, POPA(out); ●, POPA (in); ×, POPC/POPA LUVs prepared with an average diameter of 1000 Å. The inset in (B) shows the low-field part of the same data expanded for clarity.

that in mind, we prepared an SUV sample containing both POPA and POPC (5 mM each lipid). The field dependence of relaxation times for this sample is shown in Figure 5, at 22 and 30 °C, which are below and above the phase transition of 28 °C for pure POPA. At 22 °C, below the T_m for pure POPA, the acyl chains of the POPA molecules may be more ordered than the POPC chains, particularly if there is any partial phase separation in these vesicles. At 30 °C, both components should have very fluid, disordered acyl chains. At 22 °C, the ³¹P line width for POPA was 260 Hz; this narrowed to ~120 Hz for the sample at 30 °C. In contrast, the line width for POPC was essentially unchanged (120 Hz) at the two temperatures. Thus, POPA does exhibit gel-like behavior in these mixed vesicles at 22 °C. As reported previously,[7] at the higher temperature the POPA ³¹P resonance is split into two, from molecules on the inside and the outside monolayer of the vesicle.

Deconvolution of the field-dependence curves at 22 °C (Figure 5A) yields a τ_c ~6 ns for POPA and ~10 ns for the POPC species; uncertainty in the deconvolution suggests there is no statistical difference in these two values. For comparison,
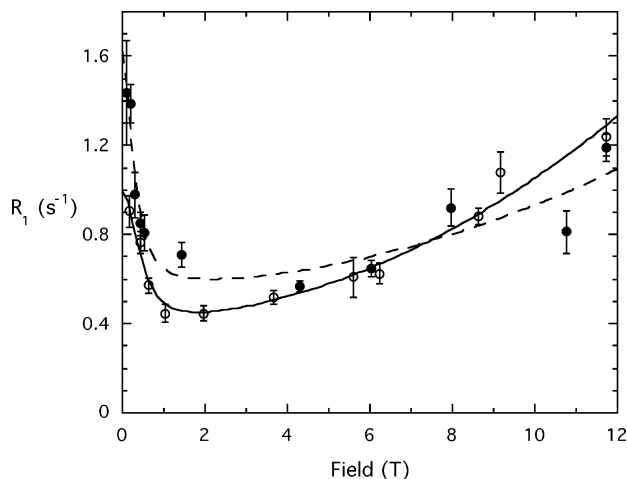
Figure 6. Comparison of field dependence for POPC in POPC/POPA SUVs at 22 °C (●) and 30 °C (○). All lines are best fits of the data to eq 1.

a value of 5 ns was observed for fluid phase DOPMe/POPC SUVs. Thus, the slower motions of the more gel-like chains of POPA do not appear to have a significant effect on the τ_c for the phosphorus group in these SUVs. More interestingly, the r_{eff} extracted from $R(0)$ is the same for POPC (2.87 Å) and POPA (2.81 Å). This indicates that the POPC choline protons and their associated motions contribute much less to the dipolar relaxation of the ^{31}P than the glycerol sn-3 CH$_2$ group.

Does this interaction change when both phospholipids are above their T_m values? For POPC in these SUVs, τ_c decreased at the higher temperature (Figure 6) and was now comparable to the value observed for POPC in POPC/DOPMe SUVs at 22 °C. As can be seen in Table 1, r_{eff} was still essentially the same for POPA and POPC at 30 °C (2.89 ± 0.02 Å). This strongly indicates that the glycerol sn-3 protons are the key players in dipolar relaxation of the phospholipid phosphorus nuclei.

Motions Reflected in τ_{hf}. Whether or not the high-field CSA contribution from internal motions reflects specific motions (rotation and isomerization), polar headgroups esterified to the phosphate[24] can be tested with the POPC/POPA SUVs. At both temperatures, the high-field rise in relaxation is smaller for POPA than it is for POPC in the same vesicle. Unfortunately, the CSA order parameter was too inaccurate or too close to one to make very useful comparisons between τ_{hf} values. However, in the one case where a comparison can be made, between POPC and the outer monolayer POPA resonance at 30 °C (Table 1), τ_{hf} is shorter for POPA. This is consistent (although not definitively so) with the proposed association of τ_{hf} with motion of the polar headgroup. Unfortunately, conclusions of this type must be viewed with caution. For example, the negatively charged PA phosphate could form a transient complex with the choline nitrogen of a neighboring molecule to slow the dynamics.

Effect of Vesicle Curvature. The chemical shift difference for POPA in each monolayer at 30 °C allows us to treat the field dependence of the two environments for POPA molecules separately. The motional parameters extracted for POPA on the inner monolayer of these vesicles had moderately large errors, and indeed, only C_H was statistically different in comparing the two resolved POPA resonances at 30 °C. However, $R(0)$, τ_c, C_L, and C_H all were increased for POPA on the inner monolayer of the vesicle (Table 1). Together these trends indicate restricted

motion for POPA packed in the inner monolayer. Previous work has shown that the ionization state of the POPA on the inner monolayer is −1, more or less regardless of external pH.[7] The tighter packing of POPA molecules in the inner monolayer dramatically raises the pK_a; it also appears to slow the motions responsible for relaxation of the phosphate group.

These SUVs are highly curved, and the curvature per se could be responsible for the motional difference of POPA on each side of the bilayer. For further insight into the motion reflected in τ_c, we examined R_1 at 30 °C and several field strengths for a preparation of LUVs prepared by extrusion from the same POPC/POPA mixture. The significantly broader line width (∼2000 Hz) for this size vesicle (average diameter ∼1000 Å) made it difficult to resolve POPA and POPC resonances, and thus an averaged R_1 was calculated from each experiment. The LUV R_1 values, plotted along with the SUV data in Figure 5B, are consistent with τ_c of 8 ns (and from that and $R(0)$, r_{eff} = 2.84 Å) and S_c^2 of 0.26, comparable to averaged τ_c and S_c^2 values for POPA (in the outer leaflet) and POPC in SUVs at this temperature. Therefore, vesicle curvature has little significant effect on the τ_c, $R(0)$, and S_c^2 that characterize dipolar and CSA relaxation of the phospholipid phosphate groups. Such behavior is consistent with our hypothesis of individual phospholipid glycerol or acyl chain reorientations and/or molecular rotation contributing to τ_c.

Structural and Dynamic Inferences from r_{eff}. The observation that r_{eff} is the same (2.8–2.9 Å) for POPA, POPC, and DOPMe (Table 1) indicates that it is the sn-3 glycerol protons that must dominate relaxation of the phosphorus nucleus. The extracted r_{eff} can be compared to r_{eff} estimated for these two protons with different dihedral angles for P−O−C−H. To estimate these distances, the 3-phosphoglycerol crystal structure with hydrogens attached was imported into the program "O", and various torsional angles varied to generate the desired P−O−C(3)−H dihedral angles. For different dihedral angles (ϕ = 0°, 60°, 120°, 180°), the P−H bond distance was estimated (2.49, 2.76, 3.21, 3.41 Å, respectively). The effective distance for dipolar relaxation of the phosphorus by these two protons a and b would be estimated by $r_{eff}^{-6} = r_a^{-6} + r_b^{-6}$. The only relationship of the protons that agrees with the value derived from field cycling is for the hydrogens to have ±120° P−O−C−H dihedral angles. For that orientation r_{eff} = 2.86 Å; for other orientations, staggered and eclipsed, at least one proton is much closer to the phosphorus and r_{eff} is ≤2.65 Å.

However, in structures of phospholipids,[28] the P−O−C−H bonds are oriented such that the two P−O−C−H hydrogens will have roughly 60° dihedral angles. For this orientation, r_{eff} should be 2.4−2.5 Å, less than our estimates in Table 1. In fact, eq 4 requires two corrections, as already mentioned, namely a factor that we estimate to be roughly 0.7 to take account of the highly anisotropic motion of the lipid and an unknown *dipolar* order parameter, S_d^2. For a true r_{eff} of 2.5 Å, appropriate for the 60° dihedral angle of the protons that relax the phosphorus, and a value for r_{eff} of 2.8 Å extracted from the analysis of field-cycling data, the product of the two corrections must be roughly 0.50, which is the sixth power of the ratio of the proposed true value and the value extracted from fitting. The dipolar order parameter would then have to be roughly 0.7 to multiply the correction for anisotropic diffusion, 0.7, and give

(28) Pascher, I. *Curr. Opin. Struct. Biol.* **1996**, *6*, 439−448.

a total correction of 0.5. This estimate is not implausible even though the amplitude of the high-frequency motion is then predicted to be in the range of 30° from its average. The acyl side chain is not held in place covalently or by strong hydrogen bonds, and it might diffuse randomly and rapidly by this much relative to the short-term average position of the anchoring acyl side chains. If this conjecture is valid, it suggests a similar value for the order parameter of the CSA interaction, S_c^2.

PI/PC Vesicles. Binary vesicles of PI and POPC (1:1) were also examined at 22 °C. Although PI has a T_m reported to be around room temperature (soybean PI, the material used here, has a T_m reported as 19−32 °C[29,30] with the actual value very dependent on buffer, salt, and pH), the ^{31}P line width (resonances for PI and PC overlap under these conditions) in these two-component vesicles was <50 Hz, suggesting a fluid bilayer. An average τ_c (and other parameters) could be evaluated (Table 1). The extracted value for $R(0)$ of 1.7 s^{-1} was significantly larger than that seen for POPC in the fluid POPC/DOPMe vesicles, while all the other parameters were within the same error as that for POPC in the POPC/DOPMe vesicles. This suggests that the inositol headgroup contains one or more inositol protons that are close enough and held sufficiently rigidly to contribute to relaxation of the phosphate. From $R(0)$ and τ_c, r_{eff} was estimated as 2.6 Å for PI, considerably smaller than r_{eff} for POPC, DOPMe, or POPA components in SUVs (Table 1; an average of r_{eff} from those three headgroups in bilayers is 2.86 ± 0.02 Å). Previous work with short-chain soluble PI molecules has shown that the inositol C(2)H displays an NOE with the glycerol sn-3 CH$_2$ group and that the inositol C(6)H is close to the phosphate group.[31] The field-cycling analysis suggests that the motion of the inositol group is likely to be restricted and that it does indeed contribute to relaxation of the ^{31}P nucleus in vesicles as well as monomer and micelle structures.

Proton Relaxation of SUVs: Segmental Motion versus Molecular Rotation. ^{1}H field cycling can also be carried out for the phospholipid proton resonances, although, in the absence of specific deuteration, chains from several species contribute to the observed proton resonances. The glycerol backbone protons, which might be expected to have properties related to those of the ^{31}P, were not resolved in the vesicle spectra and could not be analyzed. An example of the R_1 field dependence for different proton resonances is shown in Figure 7A for POPC/DOPMe SUVs at 22 °C. Different parts of the molecule were characterized by different τ_H values (see Methods). Of the resonances monitored, acyl chain protons exhibited the highest τ_H (3.1 ns for the α-CH$_2$), but this value was roughly half the τ_c for the ^{31}P nuclei in the same vesicle (5−8 ns). Polar headgroup protons exhibited the shortest τ_c with $\tau_H \approx 0.4$ ns for the methyl group in DOPMe and 0.8 ns for the POPC choline N−CH$_3$. The lower τ_H deduced from ^{1}H relaxation reflects significant segmental motions of the chains and headgroups. The POPC/POPA SUVs at 30 °C showed similar values (Figure 7B); these data are summarized in Table 2. There is a large variation in the constant term used to fit the data, which presumably reflects differences in proton−proton cross-relaxation.
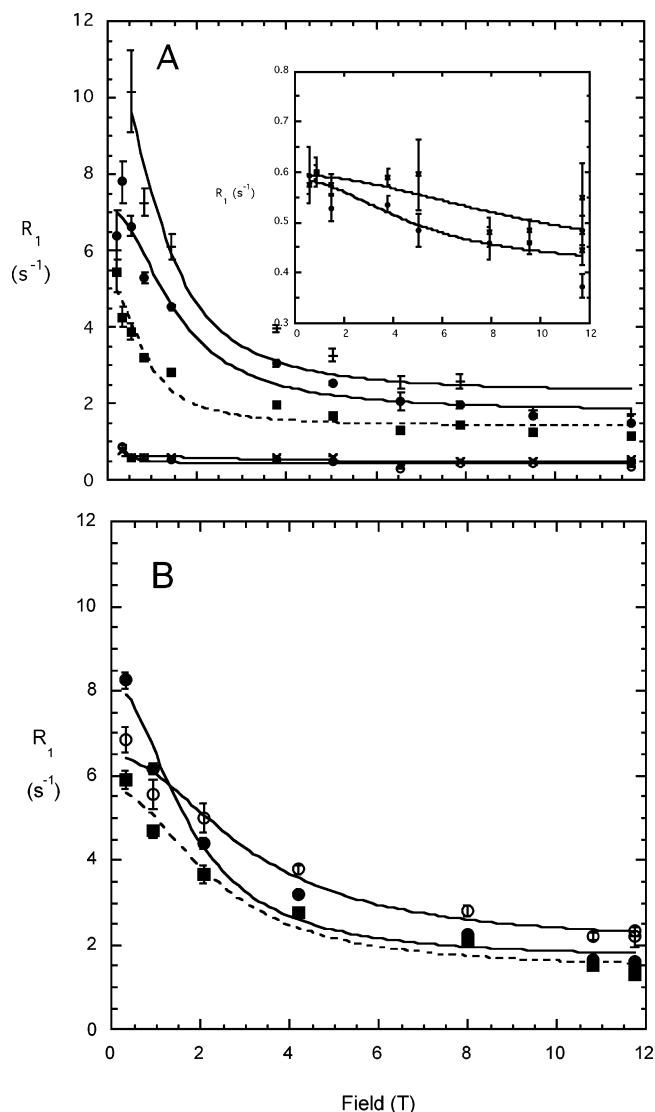
(29) Somerharju, P.; Virtanen, J.; Eklund, K.; Vainio, P.; Kinnunen, P. *Biochemistry* **1985**, *24*, 2773−2781.
(30) Egberts, J.; Sloot, H.; Mazure, A. *Biochim. Biophys. Acta* **1989**, *1002*, 109−113.
(31) Zhou, C.; Garigapati, V.; Roberts, M. F. *Biochemistry* **1997**, *36*, 15925−15931.
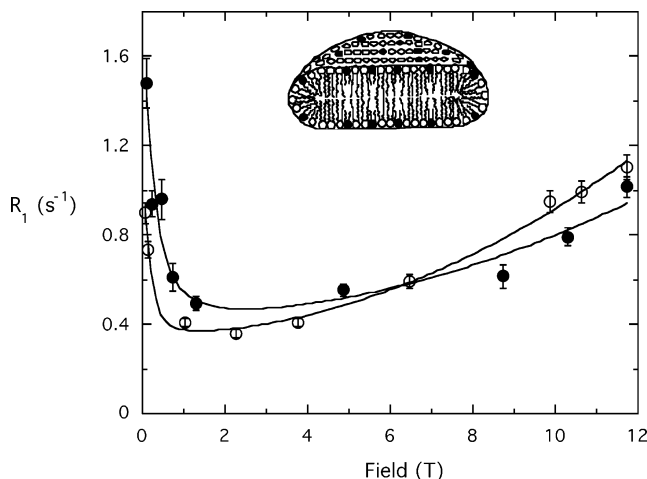

Figure 7. ^{1}H R_1 field dependence for (A) POPC/DOPMe at 22 °C and (B) POPC/POPA SUVs at 30 °C: ○, −N(CH$_3$)$_3$; ×, −OCH$_3$; +, α-CH$_2$; ●, (CH$_2$)$_n$; ■, −CH$_3$. The lines are the best fits to eq 5; the dashed lines are the fit to the alkyl chain terminal CH$_3$ relaxation. The inset shows an expanded vertical scale for the POPC (O) and DOPMe (X) methyl protons.

Table 2. Relaxation Parameters for POPC/POPA and POPC/DOPMe SUVs at 22 °C Extracted from Fitting the ^{1}H Field Dependence of R_1 to Eq 5

sample	group	τ_H (ns)	$R(0)$ (s^{-1})	c	$R(0) + c$
POPC/DOPMe	N(CH$_3$)$_3$	0.8	0.2	0.4	0.6
	−OCH$_3$	0.4	0.2	0.4	0.6
	α-CH$_2$	3.1	8.7	2.3	11.0
	(CH$_2$)$_n$	2.5	5.3	1.8	7.1
	CH$_3$	$-^a$	3.8	1.4	5.2
POPC/POPA	N(CH$_3$)$_3$	1.2	4.4	2.0	6.4
	(CH$_2$)$_n$	2.2	6.5	1.7	8.2
	CH$_3$	1.6	4.2	1.4	5.6

^{a} The field dependence of the terminal methyl R_1 is not well-fit by eq 5. However, $R(0)$ can be well-estimated. Errors in τ_H were typically <25%, with $R(0)$ errors <20% except for the α-CH$_2$ group where the uncertainty in the extracted τ_c was closer to 35%.

Dilute Bicelles. A different type of phospholipid aggregate is formed by mixing short-chain phospholipids with a long-chain saturated phospholipid below its T_m; for example, a mixture of 20 mM DPPC and 5 mM diC$_7$PC at room temperature.[32,33] The same type of mixture forms magnetically alignable

Figure 8. ^{31}P R_1 field dependence for bicelles at 22 °C: DPPC/diC$_7$PC = 4:1 (○) and 2:1 (●); the lines are the fits to eq 1. The inset depicts a bicelle with the short-chain component denoted by ● and the long-chain gel-state component as ○.

"bicelles" that have been studied in considerable detail[34,35] at high concentrations (>15 wt %) and temperatures above the long-chain phosphatidylcholine T_m. At high temperature but lower total lipid concentrations vesicles can also form,[36] which we did not study. The DPPC/diC$_7$PC mixture at room temperature will form a nearly optically clear solution of predominantly bilayer disks (although some vesicles can exist[32] with an average diameter of ~200 Å.[33] Either cooling the solution to 4 °C or increasing the temperature well above the T_m (41 °C for DPPC) causes a reversible fusion of the small dilute particles to large multilamellar structures.[37] Below the T_m, it is thought that the short-chain PC component surrounds edges of the gel-like DPPC disks in these small particles.[38] The fused structure with the long-chain phospholipid above its T_m may form a heavily perforated, highly dynamic lamellar bilayer phase, rims of holes enriched in the short-chain phospholipid.[39]

We have examined two of these solutions, 20 mM DPPC with either 5 or 10 mM diC$_7$PC (4:1 or 2:1 DPPC/diC$_7$PC) at 22 °C (Figure 8). A single broad phosphorus resonance was observed in both cases. The 4:1 DPPC/diC$_7$PC aggregates exhibited a τ_c 3-fold longer than that for most phospholipids above their T_m. The larger τ_c for the bicelles suggests that the short-chain diC$_7$PC is interacting intimately with some of the gel-like long-chain DPPC and that the relaxation behavior of both is more akin to gel-like phospholipids. The increased C_L term for bicelles also suggested a significantly increased CSA order parameter (in this case the fitted S_c^2 was greater than 1) compared to the fluid SUVs examined. As more diC$_7$PC was added to the particles, τ_c decreased, although the change was only mar-

ginally significant. However, the decrease in $R(0)$ with increasing diC$_7$PC was statistically significant. Since $R(0)$ includes in it τ_c, this strongly indicates that τ_c does indeed drop as diC$_7$PC concentration in the particles increased (from 20 to 33 mol %). The decrease in τ_c, as more diC$_7$PC is added to the system, is consistent with the short-chain component clustering together (preferentially in the edge of the particles) and achieving higher mobility in these patches (see the drawing in Figure 8). If the diC$_7$PC were merely at the edges of the bilayer, the changes in τ_c as a function of increasing the fraction of this short-chain component might be expected to be much less than this.

PI-Specific Phospholipase-C Binds and Perturbs the Motion in POPC Bilayers. The effect of molecules that bind to specific components of the SUVs can also be explored with high-resolution field cycling. The PI-specific phospholipase C (PI−PLC) from *B. thuringiensis* is a peripheral membrane protein that catalyzes the hydrolysis of PI to produce diacylglycerol and inositol-1-phosphate. The bacterial enzyme is highly activated by binding to surfaces composed of the nonsubstrate PC molecules.[40,41] Phospholipids with other headgroups (e.g., PMe) do not enhance enzyme activity.[40,42] Although the K_D for partitioning of the enzyme to anionic vesicles (under low ionic strength conditions) indicates tighter binding,[43] the interaction with the anionic vesicles is primarily electrostatic while binding to PC surfaces has a major hydrophobic character.[17]

We have examined the effect of the enzyme on single-component POPC SUVs at pH 7.5 and, likewise, single-component DOPMe SUVs as a control. The ratio of PC in the outer leaflet of these small vesicles to enzyme is in the range of 60−66 to 1. This is enough of an excess POPC that all the PI−PLC should be bound to the PC SUVs (the vesicle binding studies suggested that the enzyme interacted strongly with and covered 5−10 phospholipid molecules); PI−PLC binding to DOPMe SUVs required a bigger domain of 50−125 phospholipid molecules.[43] Filtration and centrifugation of the NMR sample after field cycling indicated that >90% of the PI−PLC was partitioned with the POPC SUVs and 50% partitioned on the DOPMe SUVs. As shown in Figure 9A, the addition of PI−PLC shifted the curve to higher $R(0)$ and changed the field for the minimum R_1. Deconvolution required only a single τ_c, indicating that the motional parameters represent an averaged value (fast exchange) of phospholipids free in the bilayer and those bound to PI−PLC. Inclusion of PLC increased the POPC $\tau_c \approx$ 2-fold, not as pronounced as the effect of cholesterol but quite substantial (Table 3). S_c^2 was also increased, from 0.46 to 0.9. Although the C_H term was not statistically different in the presence of enzyme, the value extrapolated for τ_{hf} was increased since $(1 − S_c^2)$ decreased. In contrast to the interaction of PI−PLC with POPC molecules in the vesicle, motional parameters for DOPMe SUVs (extracted from Figure 9B) were not significantly affected by the presence of the enzyme even though half of the protein was tightly associated with the vesicles under the field-cycling conditions (measured by centrifugation and filtration of the mixture after cycling[43]).

The effect of the enzyme on the vesicles containing the activating phospholipid PC is consistent with the enzyme

(32) Gabriel, N. E.; Roberts, M. F. *Biochemistry* **1987**, *26*, 2432−2440.
(33) Lin, T.-L.; Lui, C.-C.; Roberts, M. F.; Chen, S.-H. *J. Phys. Chem.* **1991**, *95*, 6020−6027.
(34) Glover, K. J.; Whiles, J. A.; Wu, G.; Yu, N.; Deems, R.; Struppe, J. O.; Stark, R. E.; Komives, E. A.; Vold, R. E. *Biophys. J.* **2001**, *81*, 2163-2171.
(35) Arnold, A.; Labrot, T.; Oda, R.; Duforc, E. *Biophys. J.* **2002**, *83*, 2667−2680.
(36) Nieh, M. P.; Harroun, T. A.; Raghunathan, V. A.; Glinka, C. J.; Katsaras, J. *Phys. Rev. Lett.* **2003**, *91*, 158105.
(37) Eum, K. M.; Riedy, G.; Langley, K.; Roberts, M. F. *Biochemistry* **1989**, *28*, 8206−8213.
(38) Luchette, P. A.; Vetman, T. N.; Prosser, R. S.; Hancock, R. E.; Nieh, M. P.; Glinka, C. J.; Krueger, S.; Katsaras, J. *Biochim. Biophys. Acta* **2001**, *1513*, 83−94.
(39) Gaemers, S.; Bax, A. *J. Am. Chem. Soc.* **2001**, *123*, 12343−12352.

(40) Zhou, C.; Wu, Y.; Roberts, M. F. *Biochemistry* **1997**, *36*, 347−355.
(41) Zhou, C.; Qian, X.; Roberts, M. F. *Biochemistry* **1997**, *36*, 10089−10097.
(42) Zhou, C.; Roberts, M. F. *Biochemistry* **1998**, *37*, 16430−16439.
(43) Wehbi, H.; Feng, J.; Kolbeck, J.; Ananthanarayanan, B.; Cho, W.; Roberts, M. F. *Biochemistry* **2003**, *42*, 9374−9382.
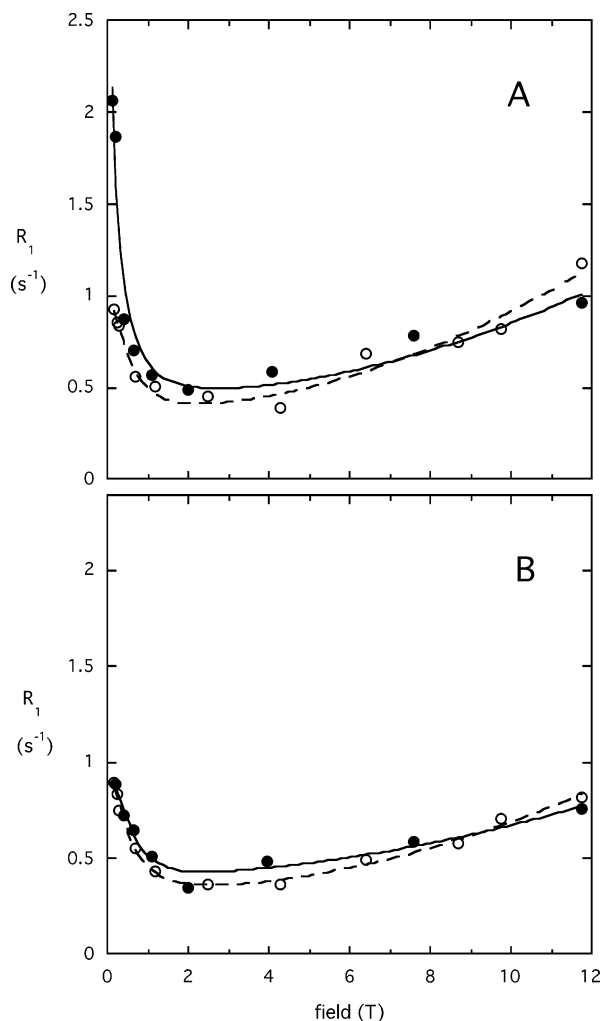
Figure 9. Effect of PI−PLC (6 mg/mL) on ^{31}P R_1 of 15 mM (A) POPC or (B) DOPMe SUVs: phospholipids in the absence (○) and presence (●) of PI−PLC. Solid lines are the fit to eq 1 with enzyme added; dashed lines are the fit in the absence of enzyme.

inserting side chains, in this case tryptophan residues,[17,44] into the bilayer. Such binding would be expected to increase the POPC τ_c and S_c^2 (and presumably τ_{hf}) since the enzyme interaction is very specific for the phosphocholine headgroup. On the other hand, the effect of the enzyme on the nonactivating vesicle DOPMe is negligible, consistent with electrostatic binding of the protein and DOPMe vesicle.[43] Electrostatic interactions between protein and negatively charged interface should not dramatically affect the rotation of individual phospholipids molecules in the bilayer unless the protein is inserted into the DOPMe bilayer.

The information on PI−PLC interactions with POPC versus DOPMe SUVs that we obtained from field cycling can be contrasted to the relatively little that is learned from a fixed field analysis carried out at 11.7 T and 22 °C. When PI−PLC was added, the POPC R_1 increased from 1.1 to 1.3 s^{-1}, with T_2 decreasing from 0.016 to 0.007 s. For DOPMe vesicles, R_1 did not change (1.10 to 1.05 s^{-1}), and neither did T_2 (0.012 to 0.013 s). Although R_1 and T_2 measured at high field are dominated by CSA relaxation, the T_2 component also has an exchange component that cannot be easily estimated with the vesicle

system. The fixed field experiment clearly shows that the PI−PLC interacts more strongly with POPC than DOPMe molecules, but it cannot quantify this interaction.

Conclusions

High-resolution ^{31}P field cycling is a new addition to the NMR techniques useful in characterizing phospholipids aggregates. To show the breadth of the technique, we have applied it to a range of systems, including multicomponent SUVs, bicelles, and protein/SUV complexes. Of the several parameters that can be extracted, the fitted parameters τ_c and r_{eff} are probably reasonably close to the actual correlation time and the true inverse sixth roots of the sum of inverse sixth powers of distances from the phosphorus to the protons. However, our estimates of the CSA order parameter S_c^2 and the high-frequency motion time-scale τ_{hf} are not satisfactory because of our ignorance of the orientation of the CSA principal axes in the membrane. Further experiments may provide sufficient information to improve these estimates without assuming a specific geometry for r_{eff}. These include, for example, studies of samples deuterated at the glycerol C3′ position to evaluate the contribution of these protons to dipolar relaxation and measurement of the motionally averaged CSA.[45] Nonetheless, for comparative purposes, the present analysis provides many insights into phospholipid structure and dynamics in vesicles and bicelles.

In the field range in which these vesicles were studied (0.1−11.7 T), there was no observed variation of ^{31}P relaxation to indicate a time scale for overall vesicle tumbling. However, time constants for two types of motion were detected: τ_c of 5−10 ns and τ_{hf} of 100−300 ps for phospholipids in fluid bilayers in the absence of additives. Phospholipid ^{31}P R_1 values have previously been found to increase with field strength, and these observations have been used to extract a correlation time for fast motion.[2,9] The wider-range field dependence shown herein indicates that the square-law dependence at high fields results from an increasing CSA contribution due to fast motion (time scale τ_{hf}). This contribution is on top of a constant CSA contribution from rotational diffusion about the membrane director with correlation time τ_c that contributes significantly to the total relaxation. This interpretation, and the fact that the dipolar component of ^{31}P relaxation is nearly nonexistent above 4 T, could not be deduced convincingly without a study of the full field dependence.

Measurements of ^2H and ^{13}C R_1 at low field in nematic liquid crystals have suggested long-range collective motions (splay and twist of the bilayer).[46,47] Such motions have been further examined by means of proton field cycling[10] and investigated by means of molecular dynamic simulations.[26] We do not believe that such collective motions are expected in our SUV samples. While low-frequency surface oscillations of the SUV membrane may exist, they seem unlikely to couple to relative phosphorus−proton motion with the required amplitude. In any case, we do not need to invoke such modes of motion to explain our results.

Correlation times for phospholipid motion in bilayers based on a variety of experimental and computational studies are summarized, in part, in Table 4. The τ_c from the analysis of

(44) Feng, J.; Bradley, W.; Roberts, M. F. *J. Biol. Chem.* **2003**, *278*, 24651−24657.

(45) Kishore, A. I.; Prestegard, J. H. *Biophys. J.* **2003**, *85*, 3848−3857.
(46) Nevzoroz, A. A.; Brown, M. F. *J. Chem. Phys.* **1997**, *107*, 10288−10310.
(47) Nevzorov, A. A.; Trouard, T. P.; Brown, M. F. *Phys. Rev. E* **1997**, *55*, 3276−3282.

Table 3. Effect of Phosphatidylinositol-Specific Phospholipase C (6 mg/mL) on Relaxation Parameters (Extracted from ^{31}P Field Dependence of R_1) for POPC or DOPMe SUVs

	POPC(15 mM)[a]	+ phospholipase C	DOPMe(15 mM)[a]	+ phospholipase C
τ_c (ns)	5.0 ± 1.4	9.3 ± 1.2	5.2 ± 0.6	3.4 ± 0.6
$R(0)$ (s^{-1})	0.96 ± 0.07	2.2 ± 0.5	0.92 ± 0.03	0.92 ± 0.07
r_{eff} (Å)	2.80	2.71	2.83	2.65
$C_L \times 10^8$	0.18 ± 0.06	0.35 ± 0.13	0.16 ± 0.02	0.12 ± 0.03
S_c^2	0.46	0.90	0.42	0.31
C_H	0.0055 ± 0.0007	0.0044 ± 0.0014	0.0038 ± 0.0003	0.0029 ± 0.0006
τ_{hf} (ps)	220	970	140	90

[a] The parameters for POPC and DOPMe in the absence of enzyme are those for each phospholipid in the 1:1 POPC/DOPMe covesicles at 22 °C.

Table 4. Comparison of τ_c Values Extracted from ^{31}P High-Resolution Field Cycling to Values for Phospholipids Aggregates Determined by Other Techniques

probe	system	τ_{slow} (ns)	τ_{fast} (ps)	interpretation	reference
^{31}P	POPC/DOPMe SUVs	5.1	160	τ_c represents molecular rotation in the bilayer and τ_{hf} wobbling within a cone	this work
^{31}P NOE	PC SUVs	1.4		internal motion	6
fluor. probe	fluid bilayer	2−5			48
^{2}H, ^{13}C	DMPC SUVs	6.7	460	wobbling and restricted wobbling of PC	47
^{13}C		1.8	7−40	τ_{fast} represents segmental motion of chains	18
^{13}C	DPPC ($>T_m$)	1.3	10−60	chain motions; wobbling in a cone for nanosecond time scale; fast internal motions arrange individual lipids into relatively cylindrical shapes	26

^{31}P field-cycling experiments is similar to so-called τ_{fast} values measured by fluorescence[48] and extracted from ^{2}H and ^{13}C analyses of dimyristoylphosphatidylcholine (DMPC) SUVs,[47] and it is slower than a τ_{slow} of 1.8 ns extracted from ^{13}C relaxation times of acyl chains.[18] Analysis of ^{1}H field-dependent relaxation data for DMPC[10] fit data to two correlation times with a ratio of 10:1 assumed; our ^{31}P field-cycling data indicate a similar ratio for the two observed relaxation times with a range in τ_c/τ_{hf} of 15−50 and a mean of 29 ± 4 for phospholipids in fluid bilayer vesicles. Although there can be argument on the motions that are responsible for a τ_c of 5−10 ns, various Brownian dynamics and molecular dynamics simulations suggest that for phospholipids in vesicles this nanosecond scale mostly reflects fluctuations in local orientation of the molecule (this could include molecular rotation about the long axis of the molecule and/or glycerol torsional motions that move the phosphate moiety) rather than much faster highly local segmental motions (see refs 26, 49 for recent reviews of advances in simulations and details on molecular motions observed during different time-scale trajectories). Moore et al.[25] examined simulations of DMPC bilayers and examined the rotational diffusion of the phosphorus to choline nitrogen (P−N) vector. The diffusion of this vector was consistent with a "crank-shaft"-type motion of the headgroup such that the overall rotation of the lipid is slightly slower than the headgroup rotation and occurs on a nanosecond time scale, comparable to what we obtained from field-cycling analysis. This could suggest that the ^{31}P NMR experiments are detecting wobble and the P−N vector motion. However, similar motional parameters are observed for PA, which has no alcohol esterified to the phosphate, and PC, suggesting that it is more likely that molecular rotation and glycerol motions dominate phosphorus relaxation.

The τ_c value for a given phospholipid (Table 1) is expected to be a good estimate of the inverse of the rotational diffusion constant of the phospholipid molecule about the membrane director axis. The magnitudes of our measurements are highly reasonable when compared to the two-dimensional transverse diffusion coefficients estimated experimentally for similar systems. The two rates must be closely related, and the relationship could be modeled theoretically. For example, in POPC at 30 °C, the latter coefficient is about 4×10^{-8} cm^2 s^{-1},[50] whereas in POPC at 22 °C we deduce a rotational diffusion constant of 2×10^8 s^{-1} from our tabulated τ_c of 5 ns for this molecule. The ratio of these rates (translation/angular) is 2×10^{-16} cm^2. This number could be compared with a random walk model for a two-legged object. Assuming a mean square step length of $\langle q^2 \rangle$ cm^2 per step and a mean square rotation size of one radian^2 per step, a naive model predicts that the above ratio should be about $\langle q^2 \rangle/2$. These numbers are thus consistent with a root-mean-square jump length of about 2 Å for lateral diffusion, which is not entirely unreasonable.

Perhaps one of the most intriguing uses of high-resolution field cycling and the ^{31}P R_1 field dependence is in monitoring motional changes in the phosphate group when soluble proteins (or other molecules) bind to vesicle components. Previous studies at moderate to high magnetic fields of proteins binding to phospholipid vesicles showed only small effects of the protein on the ^{31}P R_1. For example, cytochrome c bound to vesicles (predominantly by electrostatic interactions) caused no change in R_1 with increasing concentration of protein.[8] Another peripheral membrane protein, annexin V, interacting with PC/PA SUVs caused significant increases in R_2 but not R_1.[51] In the present work, the binding of PI−PLC to vesicles composed of a nonsubstrate activating phospholipid (POPC) had a large effect

(48) Davenport, L.; Targowski, *Biophys. J.* **1996**, *71*, 1837−1852.
(49) Dolainsky, C.; Unger, M.; Bloom, M.; Bayerl, T. *Phys. Rev. E* **1995**, *51*, 4743−4750.

(50) Berg, H. *Random Walks in Biology*; Princeton University Press: Princeton, NJ, 1983; pp 56 and 83.
(51) Swairjo, M. A.; Roberts, M. F.; Campos, M. B.; Dedman, J. R.; Seaton, B. A. *Biochemistry* **1994**, *33*, 10944−10950.

on τ_c and S_c^2 of the phospholipids, likely due to partial insertion of the protein into the bilayer. Partitioning of the enzyme to an anionic interface where binding is primarily electrostatic did not significantly affect ^{31}P motional parameters measured in our experiments. For PI−PLC, the clear differentiation of hydrophobic versus electrostatic interactions with PI−PLC in the ^{31}P NMR relaxation parameters opens up the possibility of examining mutants whose surface binding may be impaired or enhanced.[44]

JA046658K